Petrography of gypsum-bearing facies of the Codó Formation (Late Aptian), Northern Brazil

JACKSON D.S. PAZ[1] and DILCE F. ROSSETTI[2]

[1]Universidade Federal do Pará, Centro de Geociências, Campus do Guamá s/n,
66075-110 Belém, PA, Brasil
[2]INPE, Rua dos Astronautas 1758, Jardim da Granja, CP 515, 12245-970 São José dos Campos, SP, Brasil

ABSTRACT

An original and detailed study focusing the petrography of evaporites from the Late Aptian deposits exposed in the eastern and southern São Luís-Grajaú Basin is presented herein, with the attempt of distinguishing between primary and secondary evaporites, and reconstructing their post-depositional evolution. Seven evaporites phases were recognized: 1. chevron gypsum; 2. nodular to lensoidal gypsum or anhydrite; 3. fibrous to acicular gypsum; 4. mosaic gypsum; 5. brecciated gypsum or gypsarenite; 6. pseudo-nodular anhydrite or gypsum; and 7. rosettes of gypsum. The three first phases of gypsum display petrographic characteristics that conform to a primary nature. The fibrous to acicular and mosaic gypsum were formed by replacement of primary gypsum, but their origin took place during the eodiagenesis, still under influence of the depositional setting. These gypsum morphologies are closely related to the laminated evaporites, serving to demonstrate that their formation was related to replacements that did not affect the primary sedimentary structures. The pseudo-nodular anhydrite or gypsum seems to have originated by mobilization of sulfate-rich fluids during burial, probably related to halokinesis. The rosettes of gypsum, which intercept all the other gypsum varieties, represent the latest phase of evaporite formation in the study area, resulting from either intrastratal waters or surface waters during weathering.

Key words: evaporite, petrography, paleolake, sabkha, Late Aptian, São Luís-Grajaú Basin.

INTRODUCTION

Ancient evaporites are economically important as sources for salts (e.g., halite and potash) and metals (e.g., Cu, Zn, Au), and as indicators for structural traps of oil and gas (Warren 1999). These deposits are abundant in sedimentary basins located along the Brazilian continental passive margin, being particularly developed in the Aptian-Albian transition (Hashimoto et al. 1987, Uesugui 1987). The evap-

orites of the Codó Formation in the São Luís-Grajaú Basin (Fig. 1) are the only ones available for surface studies in the north equatorial Brazilian margin. Detailed facies analysis of fresh exposures in several open quarries located in the southern and eastern margins of this basin has provided elements to support a depositional system represented by a lacustrine or sabkha complex (Paz and Rossetti 2001, Rossetti et al. 2004). In addition, the deposits exposed in these localities constitute an excellent opportunity to better understand the post-depositional processes that took place after primary evaporite for-

Correspondence to: Dilce de Fátima Rossetti
E-mail: rossetti@dsr.inpe.br

mation. Such approach concerning to the Aptian evaporites from the north equatorial Brazilian margin has not been conducted yet.

A preliminary field investigation showed that the evaporites from the Codó Formation include several morphologies, suggesting they might not be all primary in origin. Petrographic studies of evaporites are useful to help deciphering their origin (e.g., Ogniben 1955, Kerr and Thompson 1963, Holliday 1970, Arakel 1980, El-Tabakh et al. 1997, Aref 1998), allowing to determine the succession of events that took place following deposition (e.g., Arakel 1980, Morad et al. 2000, Pérez et al. 2002). Thus, this type of study applied to the Codó Formation might contribute to better define and/or reconsider the proposed lacustrine/sabkha system. Deciphering the post-depositional history of these evaporites might help to decide on their potential for strontium and sulfur isotopic studies aiming to test the hypothesis of a possible marine influence during sedimentation, as previously proposed elsewhere (e.g., Rossetti et al. 2000).

GEOLOGICAL SETTING

The Gondwana split up took place through several steps, culminating in the Aptian with the break up of African and South American continents (Góes and Rossetti 2001). This process led to final establishment of several rift basins along the equatorial Brazilian margin, where the São Luís-Grajaú Basin is one of the largest, occupying 150,000 km^2. This basin has been interpreted as a unique structural feature formed by combination of pure shear stress and strike - slip deformation (Góes and Rossetti 2001). The main rifting developed in the Albian, when fault offsets reached up to 400 m (Figs. 2A, B), but initial fault displacement gave rise to a shallow and widespread basin where the Codó Formation was deposited in the Late Aptian. This unit is defined at the top by a regionally correlatable unconformity marked by an irregular, erosion surface with associated paleosol (Paz and Rossetti 2001).

Exposures of the Codó Formation include shal-

lowing-upward deposits attributed to lacustrine or saline pan-sabkha depositional environments (Paz and Rossetti 2001, Rossetti et al. 2004; Fig. 3). In the Codó area, where a lacustrine system dominates, the shallowing upward cycles consist of bituminous black shales, evaporites and, subordinately, calcimudstones attributed to central lake depositional environments. These deposits grade upward into gray to green shales and limestones (i.e., calcimudstone, laminated to massive peloidal wackestone to grainstone, and sparstone), related to intermediate lake environments. The top of the shallowing-upward cycles comprises massive pelite, shale, limestone (e.g., intraclastic grainstone, ostracodal wackestone to grainstone, ooidal to pisoidal packstone, tufa) and rhythmite of limestone and shale. These lithologies display a variety of sedimentary features consistent with marginal lake deposition, such as paleosol, karstic surface, fenestrae, meteoric cement, vadose pisoid. In the Grajáu area, a saline pan-sabkha depositional environment was proposed (Rossetti et al. 2004), being represented by evaporite and locally tufa, gray-green shale, and calcimudstone.

The evaporite facies consists of laminated gypsum (formed by alternating darker and lighter couplets that are up to 15 cm thick), gypsarenite, and massive-macronodular gypsum, which record deposition in flat lying areas, intraformational reworking of previously deposited evaporites, and remobilization of salts during burial, respectively. Laminated gypsum occurs in both of the study areas, dominating in the Grajaú area, while gypsarenite was observed only in the latter. Massive to macronodular gypsum is widespread in the Codó area, occurring mostly in the nucleus of evaporite lenses that are up to 5 m thick, which enclose chunks of black bituminous shales. In the Grajaú area, these deposits form diapiric features that are up to 6-8 m high at the outcrop scale. The contact between the massive-macrogranular gypsum and the laminated gypsum is gradational, except locally where the diapirs are well defined by sharp boundaries.
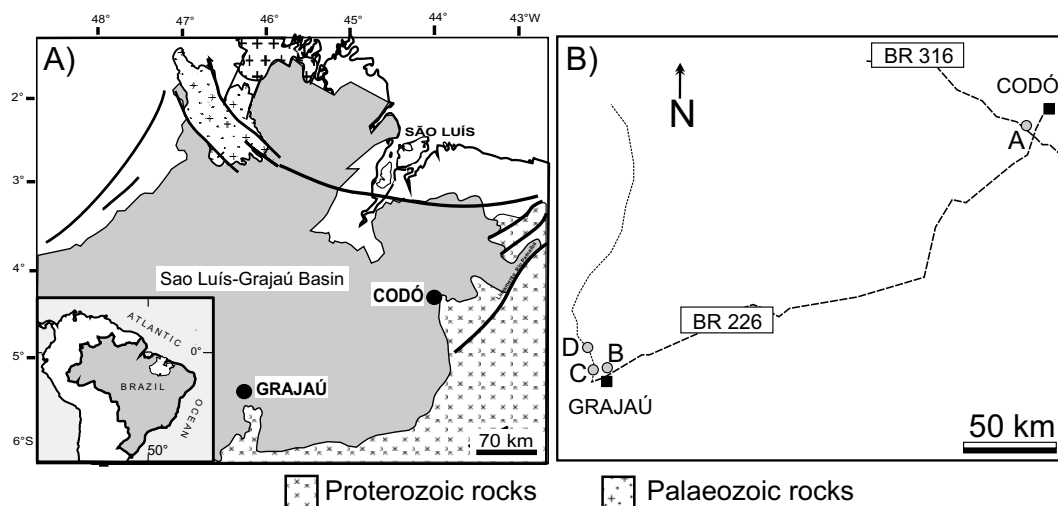
Fig. 1 – A) Location map of the study areas in the São Luís-Grajaú Basin, northern Brazil. B) A close up map, indicating the location of the studied sections in the Codó and Grajaú areas.

PETROGRAPHY OF THE EVAPORITES

The evaporite facies from the Codó Formation were characterized petrographically through the analysis of 86 thin sections distributed along four vertical sections (Fig. 4). Based on morphology and crystal relationships, eight phases of evaporite formation were recognized, which include (Fig. 5): 1. chevron gypsum; 2. nodular to lensoidal gypsum or anhydrite; 3. acicular gypsum; 4. mosaic gypsum; 5. brecciated gypsum or gypsarenite; 6. pseudo-nodular anhydrite or gypsum; and 7. rosettes of gypsum. In addition to these evaporite phases, an episode of carbonate (calcite/dolomite) cementation or replacement took place in these deposits.

Chevron Gypsum

This type of gypsum was recorded in both of the study areas, being much more widespread in sections located in the Grajaú area. The chevron gypsum, which represents the lighter component of the laminated gypsum facies, was described in a previous work, and it forms horizontal beds that are up to 10 cm thick of vertically aligned crystals. Under microscope, the chevron crystals form twin planes and superimposed growth faces with acute angles arranged as a zig-zag, perpendicularly to the crystal long axis (Fig. 6A). The chevron crystals usually grew up or are mantled by thin discontinuous layers of shales (mostly with smectites). Some thicker layers of chevron gypsum might display packages of crystals that slumped down into the muds, resulting in a series of segments with superimposed lower concave up shapes.

Nodular to Lensoidal Gypsum or Anhydrite

This evaporite was recorded only in subsurface, occurring in association with shales. It consists of either nodules of gypsum or isolated lensoidal gypsum crystals that are parallel to bedding planes (Figs. 6B,C). The nodules are up to 5 mm long, and internally composed by a dark mixture of anhydrite and gypsum that form a massive cryptocrystalline framework.

Fibrous to Acicular Gypsum

This type of gypsum occurs invariably in association with chevron gypsum, likewise forming vertically oriented crystals similar to needles (Fig. 6D). Although individual areas with dominance of
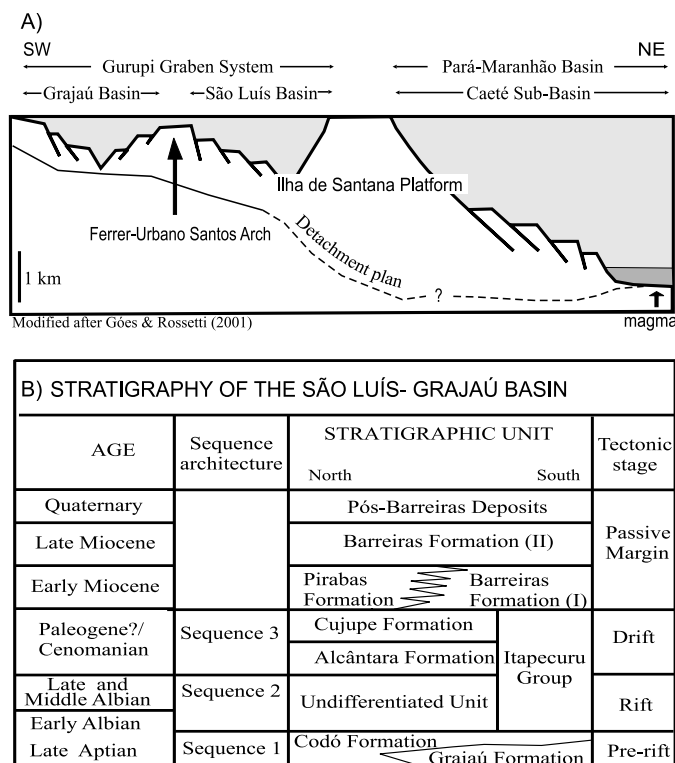
A)

Fig. 2 – A) Diagram with the sketched representation of the proposed structural pattern of the São Luís-Grajaú Basin in the Gurupi Graben System, and its relation with the Pará-Maranhão Basin. In this model, the Ferrer-Urbano Santos Arch is considered as an intrabasin horst within an abandoned intracontinental rift system formed by combination of pure shear stress and strike-slip deformation. The northeastward rifting migration through time gave rise to the development of a deeper basin, represented by the Caeté Sub-basin (cf. Góes and Rossetti 2001). B) Stratigraphic framework of the São Luís-Grajaú Basin (cf. Rossetti 2001).

fibrous and acicular gypsum were observed, in general these types of gypsum are intergraded, resulting in a closely interlaced framework. Noteworthy is the frequent presence of relics and/or ghosts of the chevron gypsum within the acicular crystals.

MOSAIC GYPSUM

This type of evaporite occurs particularly within the dark bundles of the laminated gypsum. It consists of crystals of gypsum averaging 300μm in length that are arranged into a mosaic framework. The contact between crystals is usually ragged and sutured. The mosaic gypsum typically displays an abundance of relics of floating anhydrite, forming a poikilitic texture (Fig. 6E).

BRECCIATED GYPSUM TO GYPSARENITE

This type of evaporite occurs most frequently intergrading with the mosaic gypsum within the darker bundles of the laminated gypsum facies. It consists of gypsum that occur as clasts ranging from μm to 1 cm in diameter (Figs. 7A, B). The clasts might be either angular to subangular, when a fitted texture is recognized, or rounded, forming locally a texture that is similar to gypsarenite (Figs. 7C). The clasts are surrounded by either a continuous or discontinuous dark cutan formed by a mixture of clay, organic matter and iron oxides. Under crossed polars, several clasts might display optical continuity, forming large crystals that can reach up to 3 mm
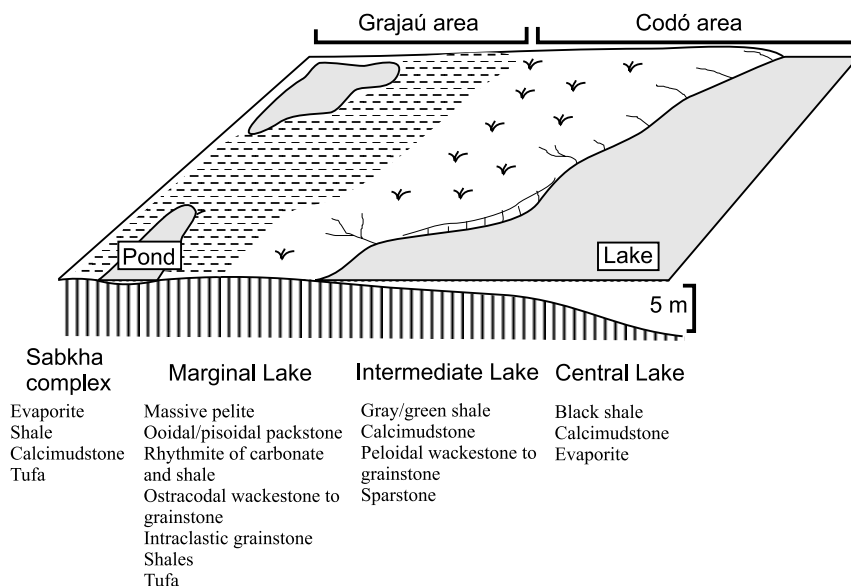
Fig. 3 – Depositional model proposed for the Codó Formation in the Codó and Grajaú areas (cf. Paz and Rossetti 2001).

of diameter (Fig. 7D). These contain abundant relics of anhydrite.

PSEUDO-NODULAR ANHYDRITE OR GYPSUM

At the outcrop scale, this consists of either slightly elongated or spherical fragments up to 5 cm long of evaporites displaying a fitted texture (Figs. 8A-C). Petrographically, the clasts are composed of alabastrine gypsum, fibrous gypsum, and anhydrite. In general, alabastrine gypsum is the most widespread, occurring as a mosaic of crystals less than 200μm in diameter (Fig. 8D). The crystals are very limpid, i.e., typically with no inclusions. The fibrous gypsum occurs secondarily as a series of parallel columns that can reach up to 1 cm long, which grew within the fractures that define the clasts, being perpendicular to fracture walls (Fig. 8A-C). Unlike to the alabastrine, the fibrous gypsum might display relics of anhydrite. In addition, ghosts of fibrous crystals are locally present within the alabastrine gypsum (Fig. 8D). In places, some elongated clasts are composed by microcrystalline lath-like anhy-drite (Fig. 8E). Where these clasts are in contact with mosaics of large gypsum crystals similar to the ones described above, the latter form concave embayments toward the anhydrites, leaving behind a "dust" of anhydrite relics (Fig. 8E). Inasmuch, both the anhydrite clasts and the mosaic gypsum might display etched margins as they grade into fibrous and alabastrine gypsum. Electronic scanning microscopic analysis of the anhydrite clasts reveals a mixture of anhydrite and limpid gypsum crystals that are similar to those observed in the nodular to lensoidal gypsum or anhydrite (Fig. 9A, compare with figure 6C). Noteworthy is that the anhydrite clasts occur as spots intergraded with alabastrine and fibrous gypsum.

ROSETTES OF GYPSUM

Rosettes of amber-colored gypsum are disperse within the evaporites of the Codó area, being restricted to the massive to macronodular gypsum (Fig. 8C). The rosettes reach up to 5 cm of diameter, and consist of fibrous crystals arranged into a
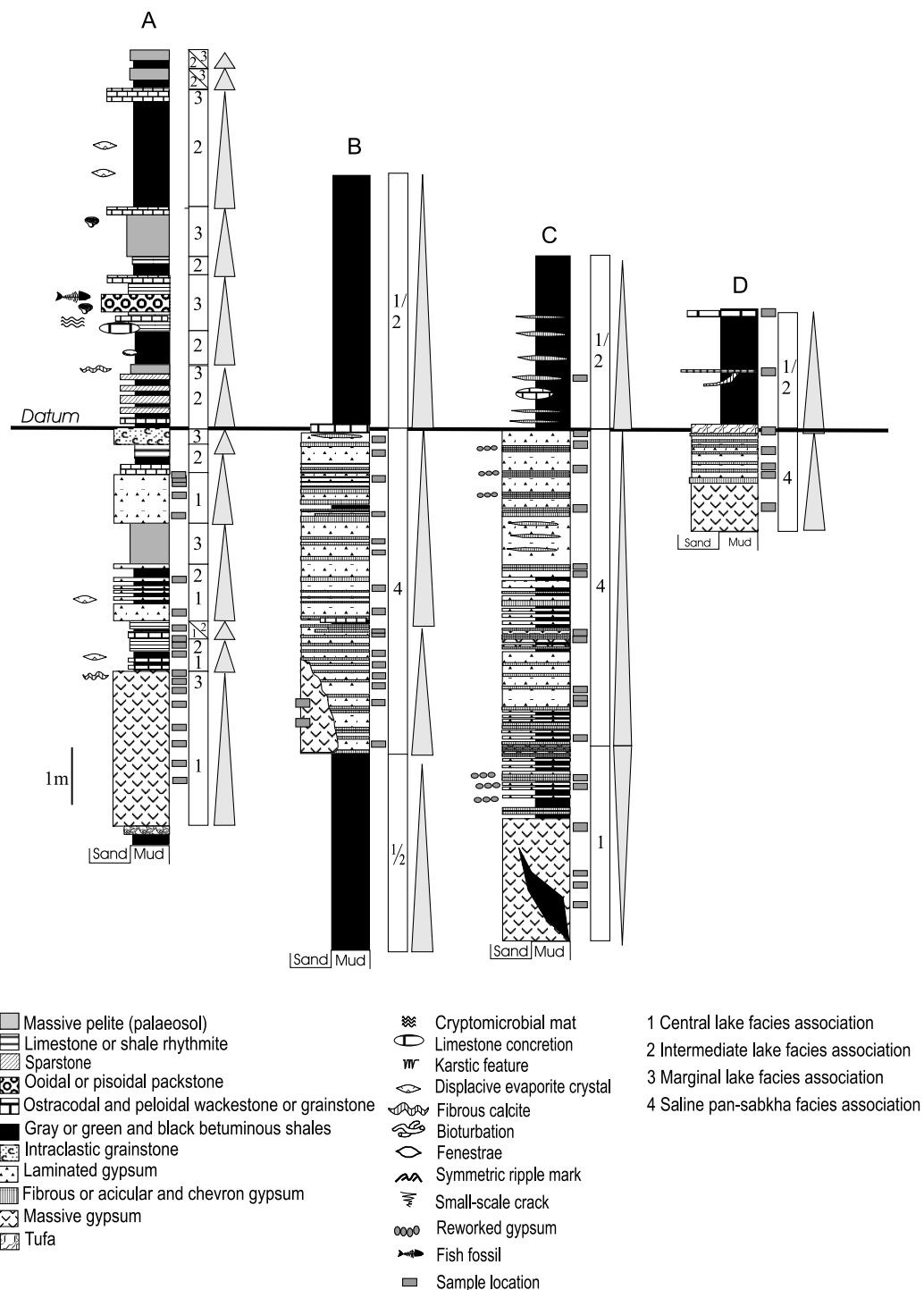
Fig. 4 – Measured vertical sections representative of the evaporites studied in the Codó Formation (see Fig. 1 for section location).

Legend (first column):
- Massive pelite (palaeosol)
- Limestone or shale rhythmite
- Sparstone
- Ooidal or pisoidal packstone
- Ostracodal and peloidal wackestone or grainstone
- Gray or green and black betuminous shales
- Intraclastic grainstone
- Laminated gypsum
- Fibrous or acicular and chevron gypsum
- Massive gypsum
- Tufa

Legend (second column):
- Cryptomicrobial mat
- Limestone concretion
- Karstic feature
- Displacive evaporite crystal
- Fibrous calcite
- Bioturbation
- Fenestrae
- Symmetric ripple mark
- Small-scale crack
- Reworked gypsum
- Fish fossil
- Sample location

Legend (third column):
1 Central lake facies association
2 Intermediate lake facies association
3 Marginal lake facies association
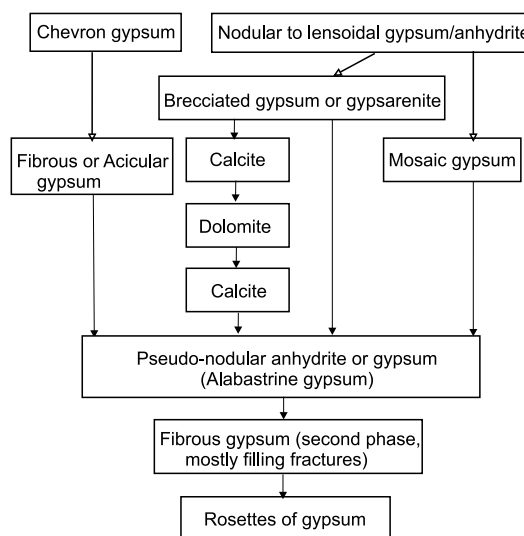4 Saline pan-sabkha facies association

Fig. 5 – The several phases of evaporites recognized in the Codó Formation, with indication of their paragenesis.

radial pattern. The rosettes unconformably cut into all the other gypsum described above.

Carbonates associated with gypsum or anhydrite consist of calcite cement that fill fractures in the brecciated gypsum or gypsarenite (Fig. 9B), even where this facies is obliterated by pseudonodular anhydrite or gypsum. The calcite also occurs as enlarged crystals that grew upon the gypsum from both sides of the fractures (Fig. 9C), in which case it forms caries in the mosaic gypsum. On the other hand, the alabastrine gypsum enters into relics of calcite, forming caries toward them (Fig. 9D). Rhombs of calcite after dolomite is locally present (Fig. 9E). Celestite might be also present in association with the carbonates, occurring as pyramidal crystals with etched edges.

PARAGENESIS

Combination of facies and petrographic characteristics revealed that the foregoing described evaporites show features supporting both primary and secondary formations. In addition, the petrographic study also showed that at least great part of the secondary gypsum might have been formed under influence of the depositional surface, thus reflecting the original brine characteristics.

Evidence for primary evaporite precipitation is particularly recorded in the laminated gypsum. We interpret that the chevron gypsum is most likely primary in origin because they make a pattern, consisting of vertically-aligned upward growing twin crystals that are similar, though in a much smaller scale, to many primary gypsum described in the literature (e.g., Schreiber and Kinsman 1975, Ciarapica et al. 1985, Hovorka 1987, Logan 1987, Handford 1991, Smoot and Lowenstein 1991, Warren 1999). In addition, the chevron gypsum is confined to the laminated gypsum, defining typical horizontal bedding planes. Important to mention also is that this gypsum forms pairs with the dark (nodular) gypsum, occurring in a very regular way throughout the sections, resulting in bundles that probably reflect seasonal brine fluctuations. Hence, the chevron gypsum would have formed under subaqueous conditions between the sediment surface and the brine due to sulfate saturation (Fig. 10A). Such feature is attributed to the progressive upward precipitation of salts on the floor of shallow (usually less than 2 m
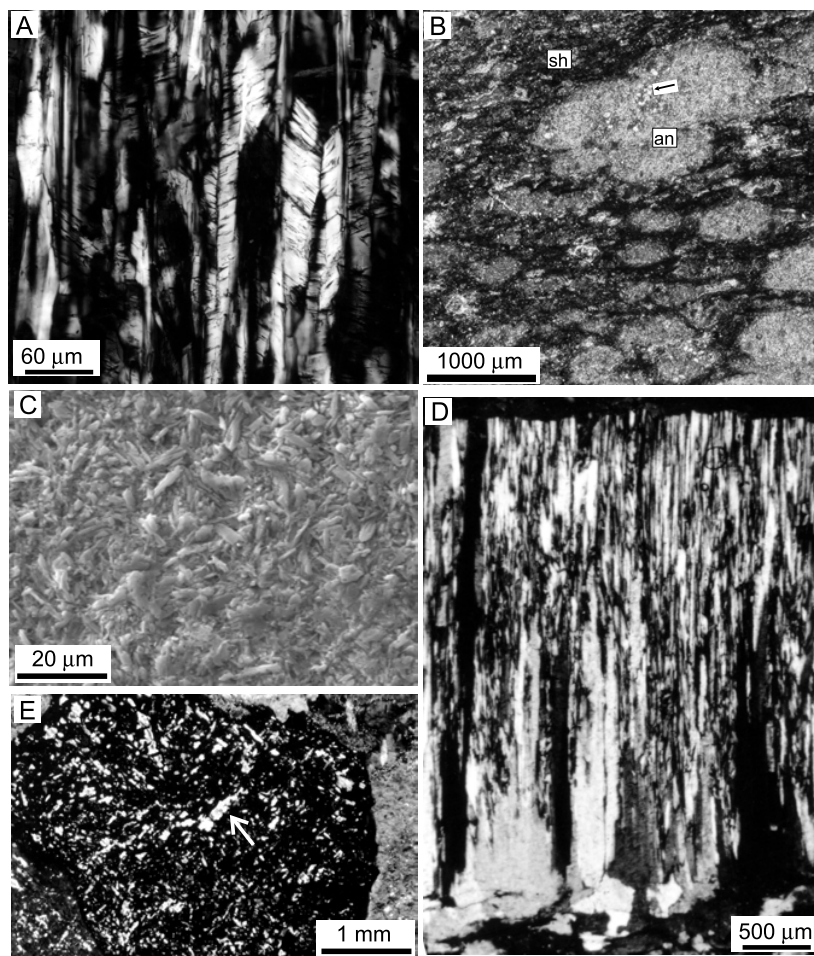
Fig. 6 – Textures of the evaporites from the Codó Formation exposed in the study areas. A) Chevron gypsum. B) Nodular gypsum (na) within bituminous black shales (sh). Note calcite relics (arrow) within nodules (crossed polars). C) A close-up of the gypsum nodules shown in figure B, illustrating their composition by micrometric, equant, lath-like crystals, typical of anhydrites. D) Acicular gypsum and, at the base, mosaic gypsum. E) Relics of anhydrite (arrow) within a large mosaic gypsum crystal. (Except for figure B, all the other figures are SEM photographs).

deep), supersatured brine pools (e.g., Logan 1987, Handford 1991, Smoot and Lowenstein 1991, Hovorka 1987), as suggested in a previous work (i.e., Rossetti et al. 2004).

Part of the light beds of the laminated gypsum is made of fibrous and acicular crystals. This gypsum morphology is similar to satin spar gypsum commonly recorded filling fractures in many publications (e.g., Richardson 1920, Shearman et al.

1972, Mossop and Shearman 1973, Stewart 1979, Gustavson et al. 1994, El-Tabakh et al. 1998). In this instance, however, the satin spar gypsum is not related to fractures but it records replacement of the chevron gypsum. This is indicated by gradation between these morphologies, and by the fact that the satin spar gypsum displays many relics and ghost of chevron gypsum. As replacement took place, the beds were slightly deformed, but still
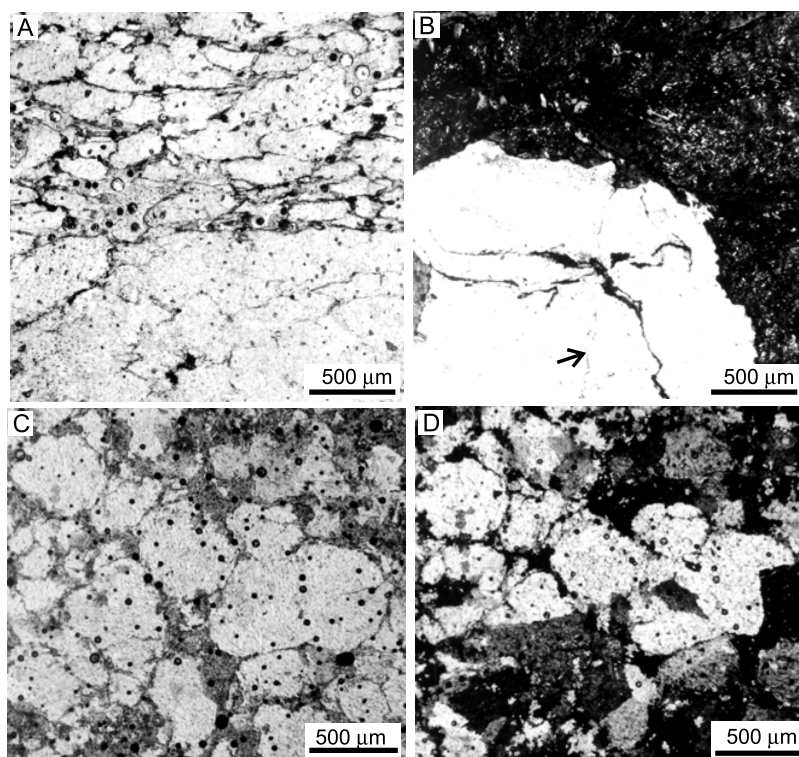
Fig. 7 – Textures of the evaporites from the Codó Formation exposed in the study areas. A) Brecciated gypsum (upper part) grading from mosaic gypsum (lower part). The dark lines around the clasts in the upper part of the photograph were formed by a mixture of muds and iron oxides, probably resulting from mechanical infiltration (parallel polars). B) Detail of the brecciated gypsum, illustrating a crystal with several fractures (arrow). Note that the optical continuity beyond fracture boundaries, attesting that fracturing occurred within a single large crystal (crossed polars). C and D) Brecciated gypsum locally displaying well rounded clasts, resembling gypsarenite (C = parallel polars; D = crossed polars). Note in D that several clasts are in optical continuity, revealing they were most likely formed by fracturing of a same large crystal.

kept the primary horizontal bedding. Although clear evidence is lacking, the absence of other types of secondary gypsum in the light gypsum beds suggests that such replacement took place shortly after deposition, thus still under a strong influence of the primary brine. Therefore, despite their authigenic nature, the satin spar gypsum is considered as a reflex of the primary evaporite bedding.

The satin spar morphology reflects crystal growth from very pure, supersaturated fluids, which favored extreme elongation parallel to the *c*-axis (Magee 1991). The close association of the acicular to fibrous gypsum with the chevron leads to suggest that formation fluids were driven from remobilization of sulfates from the chevron gypsum, whose formation naturally required high brine saturation. It is important to mention that neither of these authigenic processes were enough to destroy the primary lamination. This is taken as evidence to suggest that the formation of mosaic and acicular gypsum took place cyclically and close to the depositional surface, just shortly after formation of the individual bundles.

The darker laminated gypsum is attributed to displacive growth of crystals beneath brines derived from supersaturated pore fluids in the capillary and/
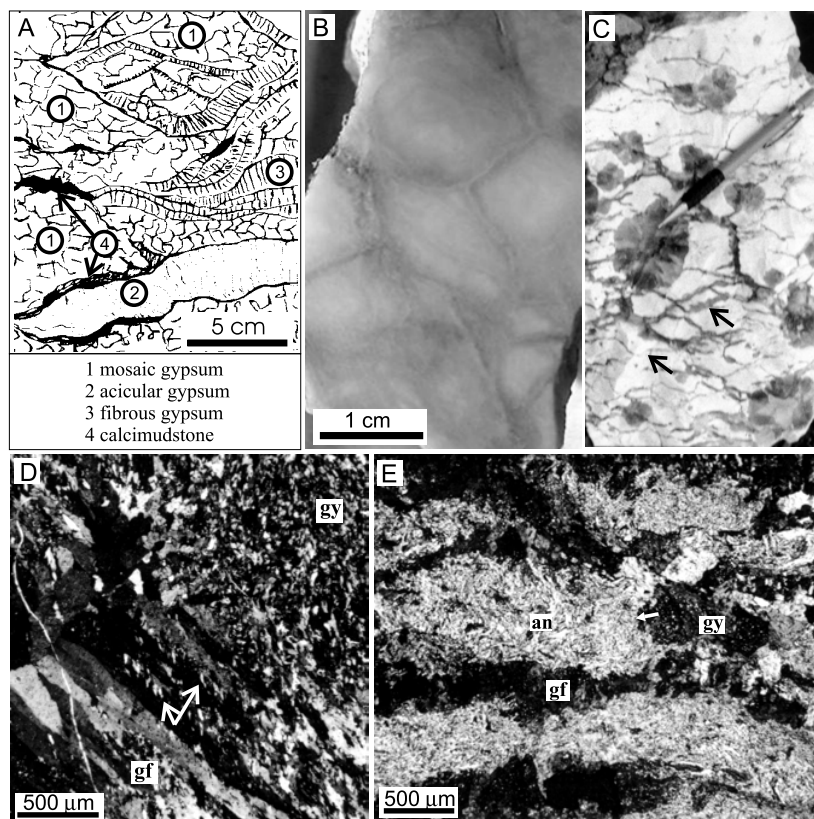
Fig. 8 – Textures of the evaporites from the Codó Formation exposed in the study areas. A) Overlay field drawing illustrating a spot within the pseudo-nodular anhydrite or gypsum with relics of a complex arrangement formed by mosaic, acicular and fibrous gypsum, bounded by films of calcimudstone. B) Pseudo-nodular gypsum, formed by fracturing (initial stage). C) A close-up of the pseudo-nodular anhydrite or gypsum, with nodules of anhydrite bound by films of fibrous gypsum (arrows). Note the superimposed rosettes of gypsum of variable sizes (rg). D) Alabastrine (gy) and fibrous (gf) gypsum in gradational contacts. The arrows indicate places where the fibrous gypsum is partly replaced by the alabastrine gypsum, recorded by numerous crystals of the later over the fibrous gypsum, which in turn remains as diffuse relics. E) A SEM view of the nodules shown in C, illustrating their composition of tiny, equant, lath-like crystals (an). Note that the edges of the nodules were replaced by fibrous (gf) or mosaic (gy) gypsum.

or upper phreatic zone (Fig. 10B). This implies periods of descending ground waters and eventual exposure (e.g., Kerr and Thompson 1963, Southgate 1982, Warren 1999). Thus, the light and dark gypsum are taken as products of high and low water level, respectively, which, given the high frequency and symmetrical distribution along the vertical sections, are most likely due to seasonal fluctuations (Figs. 10C-E).

The cyclic alternation of fibrous gypsum with dark gypsum containing nodular to lensoidal gypsum or anhydrite is also a reflex of changes in the depositional conditions. The formation of these morphologies is consistent with deposition taking place a few millimeter of the depositional surface by displacive intrasediment growth of crystals beneath the brine from supersaturated pore fluids in the capillary and/or upper phreatic zone (e.g., Kerr and Thomson 1963, Warren 1999). As the brine level decreased, nodular to lensoidal gypsum grew
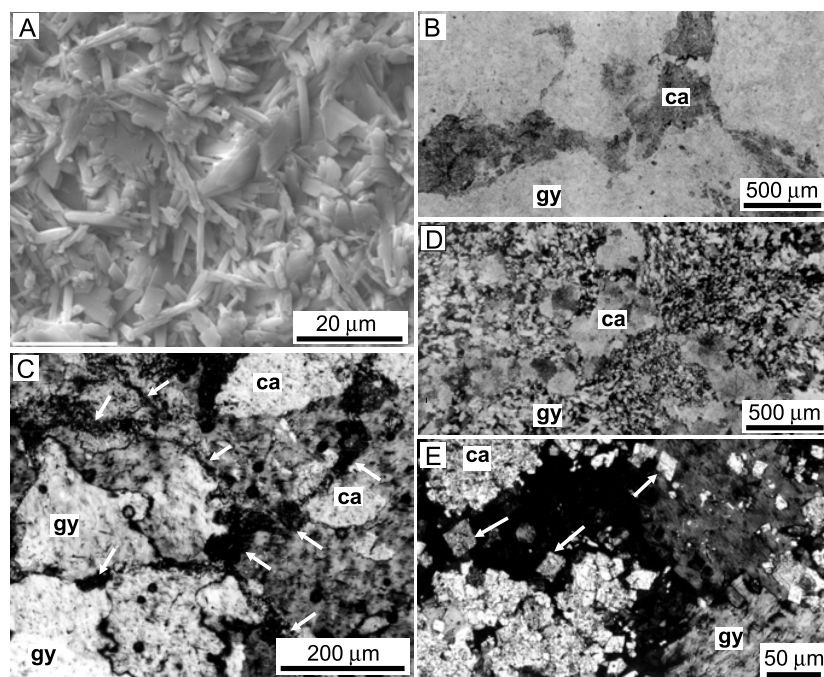
Fig. 9 – Textures of the evaporites from the Codó Formation exposed in the study areas. A) SEM view of the pseudo-nodular anhydrite or gypsum, with lath-like anhydrite (an) interlaced with gypsum (gy). This material comes from a nodule of anhydrite depicted in figure 8C. B) Calcite (ca) cementing fractures in the pseudo-nodular anhydrite or gypsum (gy). C) Detail of the pseudo-nodular anhydrite or gypsum showing several fractures (arrows) filled by a mixture of calcite and muds. Note larger calcite crystals (ca) that grew sidewards from the fractures trough replacement of gypsum (gy). D) Relics of calcite (ca) within alabastrine gypsum (gy) from the pseudo-nodular anhydrite or gypsum. E) Rhombs of calcite after dolomite (arrows). (Except for the SEM micrography shown in A, all the other figures were obtained under petrographic microscope with crossed polars).

displacively within the underlying sediments, here represented by shales. This is the most common habit of gypsum precipitated within the sediments, either in mudflats or other environments subjected to palustrine conditions (Magee 1991).

The presence of nodules composed by a dark mixture of anhydrite and gypsum forming a massive cryptocrystalline framework is consistent with this interpretation, being related to increased evaporation, probably due to climatic changes (Rossetti et al. 2004). Similar masses of mixing gypsum have been considered as the record of sulfate replacements during seasonal variations next to the depositional surface (p.e., Arakel 1980, Mees 1998, Mees and Stoops, 2003).

The mosaic gypsum was formed by replacement of anhydrite, as indicated by the abundant remains of this mineral within it. Mosaics of gypsum crystals with sutured contacts have been interpreted as a non-equilibrium texture of grain interpenetration at low temperature (cf. Voll 1960), probably reflecting formation under early diagenesis (e.g., Spencer and Lowenstein 1990). The occurrence of mosaic gypsum in association with the dark bundles, alternated with chevron to acicular gypsum within the laminated gypsum, might be taken as evidence of replacement soon after deposition.

Extreme low brine level with subaerial exposure resulted in gypsum fracturing due to desiccation, a process that gave rise to *in situ* brecciated

gypsum and ultimately gypsarenite (Fig. 10E), the latter recording local reworking at the surface as recorded in other evaporite deposits (e.g., Sanz-Rubio et al. 1999, Schreiber and El Tabakh 2000). The frequent upward gradation from the brecciated to the gypsarenite is consistent with this interpretation. The presence of mud cutans surrounding the clasts is attributed either to mechanical infiltration from downward flows or to the adhesion of residues on clast surfaces during reworking.

Following brecciation, there was a phase of widespread replacement, which gave rise to mosaics of large gypsum crystals affecting the dark beds of the laminated gypsum facies. This sequence of event is proposed based on the observation that large gypsum crystals encompass several clasts, attesting to pervasive cementation and/or replacement. The presence of abundant relics of microcrystalline lath-like anhydrite within the mosaics attests to their origin following a period of anhydrite formation. Noteworthy is the fact that the mosaics were developed only in the darker bundles of the laminated gypsum, not affecting the lighter components. Instead, the chevron gypsum was replaced, as previously mentioned, by fibrous and acicular gypsum.

Fracturing at the surface created porous, which were cemented by calcite. Calcite also replaced gypsum near the fracture sides. Under subaerial conditions (i.e., vadose to freshwater phreatic), sulfate-undersaturated pore fluids dissolve gypsum and/or anhydrite and release Ca^{2+} for precipitation of calcite as the CO_3^{2-} has more affinity with calcium than with SO_4^{2-} (cf. Back et al. 1983). Rare dolomite rhombs might have been formed either by replacement of calcite or simultaneous dolomite precipitation. The dolomite was in turn replaced by calcite. Dedolomitization is closely linked to karstification (Cañaveras et al. 1996). This process might have contributed to release Sr^{2+}, which combined with SO_4^{2-}, promoted precipitation of celestite (cf. Olaussen 1981, Taberner et al. 2002). The celestite formation, in turn, also releases Ca^{2+} that increases the Ca/Mg ratio, and could have dissolved dolomite
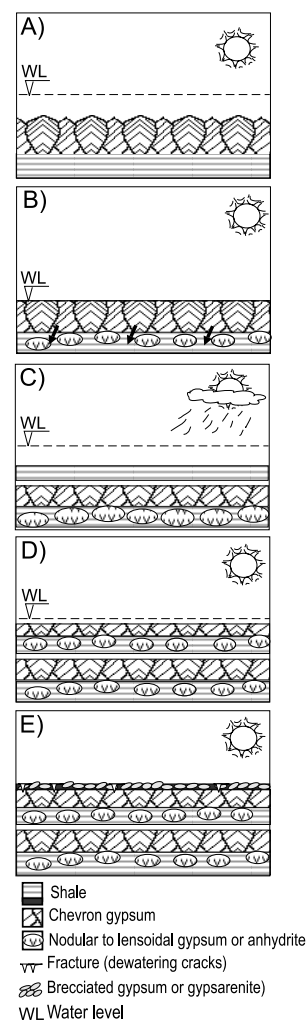

Fig. 10 – A model explaining the formation of the light and dark bundles in the laminated gypsum facies, as well as brecciated gypsum or gypsarenite. A) Brine concentration led to growth of vertically-aligned chevron gypsum in the interface between the sediment and the brine. B) During low water level, sulfate-rich descending flows resulted in the origin of displacive gypsum, forming nodular to lensoidal gypsum or anhydrite within the sediment. C) Renewed phase of higher water level promoted mud deposition. D) The increase in salt concentration due to evaporation gave rise to a renewed phase of fibrous gypsum formation. E) Extreme evaporation led to the eventual subaerial exposure of the depositional surface, brecciation and reworking of previously deposited evaporites, with the consequent formation of brecciated gypsum or gypsarenite facies.

and renewed calcite precipitation (p.e., Back et al. 1983, Kushnir 1985). The close association of calcite, dolomite and celestite in the studied evaporites of the Codó Formation suggests these processes as the most likely.

The pseudonodular anhydrite or gypsum is interpreted to represent a later phase of gypsum formation. First, this is suggested by its occurrence restricted to the massive to macronodular gypsum, where primary sedimentary structures were almost entirely lost. The presence of massive gypsum grading into the laminated gypsum, and the diapiric geometry enclosing chunks of black bituminous shales is related to salt remobilization during halokinesis. Second, the pseudonodular anhydrite or gypsum contains limpid alabastrine and fibrous crystals, not observed in association with the laminated gypsum, which is consistent with the proposed late formation. Fine crystalline gypsum have been considered as secondary in origin (Holliday 1970), forming in consequence of hydration, especially of anhydrite, induced by diapirism or other mechanism that allow percolation of water through evaporite rocks (Holliday 1970, Warren 1999). Fracturing seems to have been the cause of the pseudonodular aspect of this gypsum. Under stress, probably related to salt remobilization, part of the gypsum might have had a ruptile behavior, ultimately breaking apart to form individual fragments (e.g., Marco et al. 2002). Saturated fluids percolating along the secondary porosity created by this process would have promoted precipitation of the fibrous gypsum. In the following, there might have had the enlargement of the fractures due to forcing caused by crystal growth. While this process took place, most of the primary sedimentary features, as well as the previous phases of evaporites, became obliterated. As the salt became mobile, there was a pervasive development of alabastrine gypsum. The later nature of this phase of gypsum is revealed by its limpid aspect, free of anhydrite inclusions, and by the fact that it contains ghosts of fibrous gypsum.

The spots with microcrystalline lath-like anhydrite that occur within the macronodular gypsum is probably a relic of one of the earliest phase of evaporite precipitation in the study area. The paragenesis reconstituted with basis on petrographic relationships shows that these anhydrites form nodules that were in part replaced by the mosaic gypsum, as revealed by the fact that the later form concave embayments that enter into the anhrydrite. The margins of this gypsum are, in turn, ragged due to reaction with fibrous and alabastrine gypsum. These relationships support that the anhydrite nodules had an early development relative to all other gypsum phases present in the pseudonodular gypsum. If so, then it is possible that the anhydrite is temporally related to the anhydrite formed in the dark bundles of the laminated gypsum, which represents one of the earliest evaporite phases developed in the Codó Formation.

The final phase of evaporite formation is recorded by the rosettes of gypsum, as confirmed by the fact that these truncate all the other evaporite morphologies. Aggregates of large fibrous gypsum crystals forming rosettes similar to the ones of the study area have been attributed to the action of either intrastratal waters during burial or surficial waters during weathering (e.g., Shearman 1966, Holliday 1970, Warren 1999).

CONCLUSIONS

Despite the many varieties of evaporites recorded in the Codó Formation exposed in the eastern and southern margin of the Grajaú Basin, these deposits display many petrographic and faciological attributes that are consistent with an early formation, either by primary precipitation or early replacements when the sediments were still under influence of the depositional surface. These types of evaporites prevail particularly in the Grajaú area, where laminated gypsum facies dominates. In both areas, burial phases of gypsum seem to have developed only where gypsum was remobilized during halokinesis.

The lack of significant deep diagenetic modification of the Codó Formation is recorded also by

studies focusing the limestones and shales interbed-
ded with the evaporites. The limestones are domi-
nated by calcimudstones and peloidal wackestones
or packstones with only local evidences of cementa-
tion or replacement. These lithologies usually dis-
play primary features, as normal grading and hori-
zontal crenulated lamination. Inasmuch, the shales
associated with the evaporites consist almost en-
tirely of smectite, with only subordinate kaolinite
and illite. Among these clay minerals, smectite is
far the dominant one, being represented by detri-
tal flakes, while the kaolinite and illite are mostly
authigenic, being related to pedogenetic horizons
(D.G. de-Freitas, unpublished data). These data are
consistent with the proposition that burial did not
cause significant textural or mineralogical modifi-
cation of the Codó Formation.

The petrographic studies presented here
strongly motivate to undertake isotopic studies in
the evaporites of the Codó Formation. The analy-
sis should be carried out using samples from the
laminated facies only, which preserves evaporites
formed both primarily and shortly after deposition,
providing information on original brine characteris-
tics. On the other hand, the pseudo-nodular anhy-
drite or gypsum and the rosettes of gypsum should
not be considered for this type of studies, as they
represent later stages of gypsum formation due to
deeper salt remobilization. Inasmuch, the spots of
anhydrite within the pseudo-nodular anhydrite or
gypsum should be also discarded in these analy-
ses. Despite the interpretation that these evaporites
might have formed contemporaneously to the early-
formed nodular to lensoidal anhydrite, the micro-
scopic studies revealed they were strongly replaced
by limpid, alabastrine gypsum, being inappropriate
for isotopic analysis that can be used for paleoenvi-
ronmental purposes.

RESUMO

Neste trabalho, é apresentado um estudo original e deta-
lhado enfocando os aspectos petrográficos dos evaporitos
de depósitos aptianos superiores expostos no sul e leste
da Bacia de São Luís-Grajaú. O objetivo é o estabele-
cimento de critérios que permitam distinguir entre eva-
poritos primários e secundários, além da reconstrução de
sua evolução pós-deposicional. Sete fases de evaporitos
foram reconhecidas: 1. gipsita em chevron; 2. gipsita ou
anidrita nodular a lenticular; 3. gipsita fibrosa a acicular;
4. gipsita em mosaico; 5. gipsita brechada a gipsarenito;
6. anidrita ou gipsita pseudo-nodular; e 7. gipsita em
rosetas. As três primeiras fases apresentam característi-
cas petrográficas condizentes com origem primária. A
gipsita fibrosa a acicular e a gipsita em mosaico foram
formadas por substituições de gipsita primária, com ori-
gem provável nos estágios iniciais da diagenêse, portanto
ainda sob influência do ambiente deposicional. Estas
morfologias de gipsita estão relacionadas com a fácies
de evaporito laminado, tendo sido formadas por substi-
tuição, porém sem afetar a estruturação primária. A gip-
sita ou anidrita pseudo-nodular originou-se pela mobili-
zação de soluções sulfatadas durante ou após soterramen-
to, provavelmente associada à halocinese. A gipsita em
rosetas, que intercepta todas as outras variedades de gip-
sita, representa o ultimo estágio de formação de evaporitos
na área de estudo, tendo resultado de soluções intraes-
tratais ou de águas superficiais durante intemperismo.

Palavras-chave: evaporito, petrografia, paleolago,
sabkha, Neoaptiano, Bacia de São Luís-Grajaú.

REFERENCES

ARAKEL AV. 1980. Genesis and diagenesis of Holocene
    evaporitic sediments in Hutt and Leeman lagoons,
    western Australia. J Sed Petrol 50: 1305–1326.

AREF MAM. 1998. Holocene stromatolites and micro-
    bial laminites associated with lenticular gypsum in a

marine-dominated environment, Ras El Shetan Area, Gulf of Aqaba, Egypt. Sedimentology 45: 245–262.

BACK W, HANSHAW BB, PLUMMER LN, RAHN PH, RIGHTMIRE CT AND RUBIN M. 1983. Process and rate of dedolomitization: mass transfer and ^{14}C dating in a regional carbonate aquifer. Geol Soc Am Bull 94: 1414–1429.

CAÑAVERAS JC, SÁNCHEZ MORAL S, CALVO JP, HOYOS M AND ORDOÑEZ S. 1996. Dedolomites associated with karstification: An example of early dedolomitization in lacustrine sequences from the Tertiary Madrid Basin, Central Spain. Carb and Evap 11: 85–103.

CIARAPICA G, PASSERI L AND SCHREIBER C. 1985. Una proposta di calssificazione delle evaporiti solfatiche. Geol Rom 24: 219–232.

EL-TABAKH M, RICCIONI R AND SCHREIBER BC. 1997. Evolution of Late Triassic rift basin evaporites (Passaic Formation); Newark Basin, eastern North America. Sedimentology 44: 767–790.

EL-TABAKH M, SCHREIBER BC AND WARREN JK. 1998. Origin of fibrous gypsum in the Newark Rift Basin, eastern North America. J Sed Res 68: 88–99.

GÓES AM AND ROSSETTI DF. 2001. Gênese da Bacia de São Luís-Grajaú, Meio-Norte do Brasil. In: ROSSETTI DF, GÓES AM and TRUCKENBRODT W (Eds), O Cretáceo na Bacia de São Luís-Grajaú, Belém: Museu Paraense Emílio Goeldi, Coleção Friedrich Katzer, p. 15–29.

GUSTAVSON TC, HOVORKA S AND DUTTON AR. 1994. Origin of satin spar veins in evaporite basins. J Sed Res A64: 88–94.

HANDFORD CR. 1991. Marginal marine halite: sabhkas and salinas. In: MELVIN JD (Ed), Evaporites, Petroleum and Mineral Resources, Amsterdam: Developments in Sedimentology 50: 1–66.

HASHIMOTO AT, APPI CJ, SOLDAN AL AND CERQUEIRA JR. 1987. O Neo-Alagoas nas bacias do Ceará, Araripe e Potiguar (Brasil): caracterização estratigráfica e paleoambiental. Rev Bras Geoc 17: 118–122.

HOLLIDAY DW. 1970. The petrology of secondary gypsum rocks: a review. J Sed Petrol 40: 734–744.

HOVORKA SD. 1987. Depositional environments of marine-dominated bedded halite, Permian SanAndres Formation, Texas. Sedimentology 34: 1029–1054.

KERR SD AND THOMPSON A. 1963. Origin of nodular and bedded anhydrite in Permian shelf sediments, Texas and New Mexico. Am Assoc Petrol Geol Bull 47: 1726–1732.

KUSHNIR SV. 1985. The epigenetic celestite formation mechanism for rocks containing CaSO$_4$. (Translation from Scripta Technica, Inc.) Geokhimiya 10: 1455–1463.

LOGAN BW. 1987. The Lake MacLeod Evaporite Basin, Western Australia-Holocene Environments, Sediments, and Geological Evolution. Am Assoc Petrol Geol Memoir 44: 140.

MAGEE JW. 1991. Late Quaternary lacustrine, groundwater, Aeolian and pedogenic gypsum in the Prungle Lakes, southeastern Australia. Palaeogeogr Palaeoclimatol Palaeoecol 84: 3–42.

MARCO S, WEINBERGER R AND AGNON A. 2002. Radial fractures formed by a salt stock in the Dead Sea Rift, Israel. Terra Nova 14: 288–294.

MEES F. 1998. The alteration of glauberite in lacustrine deposits of the Taoudenni-Agorgott basin, northern Mali. Sed Geol 117: 193–205.

MEES F AND STOOPS G. 2003. Circumgranular bassanite in a gypsum crust from eastern Algeria – a potential palaeosurface indicator. Sedimentology 50: 1139–1145.

MORAD S, KETZER JM AND DE ROS LF. 2000. Spatial and temporal distribution of diagenetic alterations in siliciclastic rocks: implications for mass transfer in sedimentary basins. Sedimentology 47 (Suppl 1): 95–120.

MOSSOP GD AND SHEARMAN DJ. 1973. Origin of secondary gypsum rocks. Trans Inst Min Metall B82: 147–154.

OGNIBEN L. 1955. Inverse graded bedding in primary gypsum of chemical deposition. J Sed Petrol 25: 273–281.

OLAUSSEN S. 1981. Formation of celestite in the Wenlock, Oslo region Norway – evidence for evaporitic depositional environments. J Sed Petrol 51: 37–46.

PAZ JDS AND ROSSETTI DF. 2001. Reconstrução paleoambiental da Formação Codó (Aptiano), borda leste da Bacia do Grajaú, MA. In: ROSSETTI DF, GÓES AM AND TRUCKENBRODT W (Eds), O Cretáceo na Bacia de São Luís-Grajaú, Belém: Museu Paraense Emílio Goeldi, Coleção Friedrich Katzer, p. 77–101.

PÉREZ A, LUZÓN A, ROC AC, SORIA AR, MAYAYO MJ AND SÁNCHEZ JA. 2002. Sedimentary facies distribution and genesis of recent carbonate-rich saline lake: Gallocanta Lake, Iberian Chain, NE Spain. Sed Geol 148: 185–202.

RICHARDSON WA. 1920. The fibrous gypsum of Nottinghamshire. Min Mag 91: 77–95.

ROSSETTI DF. 2001. Arquitetura deposicional da Bacia de São Luís-Grajaú, meio norte do Brasil. In: ROSSETTI DF, GÓES AM AND TRUCKENBRODT W (Eds), O Cretáceo na Bacia de São Luís-Grajaú, Belém: Museu Paraense Emílio Goeldi, Coleção Friedrich Katzer, p. 31–46.

ROSSETTI DF, PAZ JDS, GÓES AM AND MACAMBIRA M. 2000. A marine versus non-marine origin for the Aptian-Albian evaporites of the São Luís and Grajaú basins, Maranhão State (Brazil) based on sequential analysis. Rev Bras Geoc 30: 642–645.

ROSSETTI DF, PAZ JDS AND GÓES AM. 2004. Facies analysis of the Codó Formation (Late Aptian) in the Grajaú Area, Southern São Luís-Grajaú Basin. An Acad Bras Cienc 76: 791–806.

SANZ-RUBIO E, HOYOS M, CALVO JP AND ROUCHY JM. 1999. Nodular anhydrite growth controlled by pedogenic structures in evaporite lake formations. Sed Geol 125: 195–203.

SCHREIBER BC AND EL TABAKH M. 2000. Deposition and early alteration of evaporites. Sedimentology 47 (Suppl 1): 215–238.

SCHREIBER BC AND KINSMAN DJ. 1975. New observations on the Pleistocene evaporites of Montallegro, Sicily and a modern analog. J Sed Petrol 45: 469–479.

SHEARMAN DJ. 1966. Origin of marine evaporites by diagenesis. Inst Min Metal Trans (Section B) 75: 208–215.

SHEARMAN DJ, MOSSOP G, DUNSMORE H AND MARTIN M. 1972. Origin of gypsum veins by hydraulic fracture. Trans Inst Min Metall 81B: 149–155.

SMOOT JP AND LOWENSTEIN TK. 1991. Depositional environments of non-marine evaporites. In: MELVIN JL (Ed), Evaporites, petroleum and mineral resources, Amsterdam: Elsevier, p. 189–347.

SOUTHGATE PN. 1982. Cambrian skeletal halite crystals and experimental analogues. Sedimentology 29: 391–407.

SPENCER RJ AND LOWENSTEIN TK. 1990. Evaporites. In: MACILREATH IA AND MORROW DW (Eds), Diagenesis. St. Johns, New Foundlands, Geosciences Canada Reprint Series 4: 141–163.

STEWART AJ. 1979. A barred-basin marine evaporite in the upper Proterozoic of the Amadeus Basin, central Australia. Sedimentology 26: 33–62.

TABERNER C, MARSHALL JD, HENDRY JP, PIERRE C AND THIRLWALL MF. 2002. Celestite formation, bacterial sulphate reduction and carbonate cementation of Eocene reefs and basinal sediments (Igualada, NE Spain). Sedimentology 49: 171–190.

UESUGUI N. 1987. Posição estratigráfica dos evaporitos da Bacia de Sergipe-Alagoas. Rev Bras Geoc 17: 131–134.

VOLL G. 1960. New work on petrofabrics. Liverpool and Manchester Geol J 2: 503–567.

WARREN J. 1999. Evaporites. Oxford, Blackwell Science, 438 p.